



Article

Spatial distributions of *Tribrachidium*, *Rugoconites*, and *Obamus* from the Ediacara Member (Rawnsley Quartzite), South Australia

Phillip C. Boan* , Scott D. Evans , Christine M. S. Hall , and Mary L. Droser

Abstract.—The spatial distribution of in situ sessile organisms, including those from the fossil record, provides information about life histories, such as possible dispersal and/or settlement mechanisms, and how taxa interact with one another and their local environments. At Nilpena Ediacara National Park (NENP), South Australia, the exquisite preservation and excavation of 33 fossiliferous bedding planes from the Ediacara Member of the Rawnsley Quartzite reveals in situ communities of the Ediacara Biota. Here, the spatial distributions of three relatively common taxa, *Tribrachidium*, *Rugoconites*, and *Obamus*, occurring on excavated surfaces were analyzed using spatial point pattern analysis. *Tribrachidium* have a variable spatial distribution, implying that settlement or post-settlement conditions/preferences had an effect on populations. *Rugoconites* display aggregation, possibly related to their reproductive methods in combination with settlement location availability at the time of dispersal and/or settlement. Additionally, post-settlement environmental controls could have affected *Rugoconites* on other surfaces, resulting in lower populations and densities. Both *Tribrachidium* and *Rugoconites* also commonly occur as individuals or in low numbers on a number of beds, thus constraining possible reproductive strategies and environmental/substrate preferences. The distribution of *Obamus* is consistent with selective settlement, aggregating near conspecifics and on substrates of mature microbial mat. This dispersal process is the first example of substrate-selective dispersal among the Ediacara Biota, thus making *Obamus* similar to numerous modern sessile invertebrates with similar dispersal and settlement strategies.

Resumen.—La distribución espacial de los organismos sésiles in situ, incluyendo los del registro fósil, brinda información sobre las historias de vida, tal como los posibles mecanismos de dispersión y/o asentamiento, y sobre cómo los taxones interactúan entre sí y entre sus entornos locales. En el Parque Nacional Nilpena Ediacara (NENP), Australia Meridional, la excelente preservación y excavación de 33 planos de lecho fosilífero del Miembro Ediacara de la Cuarcita Rawnsley revela comunidades in situ de la biota ediacárica. En este estudio analizamos las distribuciones espaciales de tres taxones relativamente comunes, *Tribrachidium*, *Rugoconites* y *Obamus*, que se encuentran en superficies excavadas mediante el análisis de patrones de puntos espaciales. *Tribrachidium* tiene una distribución espacial variable, lo que implica que las condiciones/preferencias durante o después del asentamiento tuvieron un efecto en las poblaciones. *Rugoconites* muestran agregación, posiblemente relacionado con sus métodos reproductivos en combinación con la disponibilidad de lugares de asentamiento en el momento de la dispersión y/o asentamiento. Además, los controles ambientales posteriormente al asentamiento podrían estar afectando a *Rugoconites* en otras superficies, lo que resultaría en poblaciones y densidades más bajas. Tanto *Tribrachidium* como *Rugoconites* ocurren como individuos en varios lechos, restringiendo las posibles estrategias reproductivas y las preferencias ambientales/de sustrato. La distribución de *Obamus* es consistente con un asentamiento selectivo, agregando cerca de sus congéneres y sobre sustratos de tapete microbiano maduro. Este proceso de dispersión es el primer ejemplo de dispersión selectiva de sustrato entre la biota ediacárica, lo que hace que *Obamus* sea similar a numerosos invertebrados sésiles modernos con estrategias similares de dispersión y asentamiento.

Phillip C. Boan, Christine M. S. Hall, and Mary L. Droser. Department of Earth and Planetary Sciences, University of California, Riverside, Riverside, California 92521, U.S.A. E-mail: pboan001@ucr.edu, csol001@ucr.edu, droser@ucr.edu

Scott D. Evans. Earth, Ocean, and Atmospheric Sciences, Florida State University, Tallahassee, Florida 32304, U.S.A. E-mail: sdevans@fsu.edu

Accepted: 1 February 2023

*Corresponding author.

Introduction

Fossil assemblages of the soft-bodied Ediacara Biota represent Earth's earliest record of complex multicellular ecosystems. There is

general consensus that the Ediacara Biota includes stem-group poriferans, cnidarians, and bilaterians (Erwin and Valentine 2013; Erwin 2015, 2021; Cunningham et al. 2017;

Bobrovskiy et al. 2018; Evans et al. 2020b, 2021a; Dunn et al. 2021, 2022), but most individual taxa remain enigmatic. Despite this, paleobiological and paleoecological studies have revealed information regarding these early organisms, including the nature of their growth (e.g., Dunn et al. 2018; Evans et al. 2021b), reproduction (e.g., Droser and Gehling 2008; Darroch et al. 2013; Hall et al. 2015; Mitchell et al. 2015), and modes of obtaining nutrition (e.g., LaFlamme et al. 2009; Rahman et al. 2015; Darroch et al. 2017; Gibson et al. 2019, 2021). The common in situ preservation of fossils of the Ediacara Biota has also allowed for examination of the spatial distributions of fossil communities, providing a dataset, unusual for the fossil record, that can be used to test hypotheses about life histories (Clapham et al. 2003; Hall et al. 2015; Mitchell et al. 2015, 2018, 2020, 2022; Coutts et al. 2018; Gehling and Droser 2018; Mitchell and Butterfield 2018; Mitchell and Kenchington 2018; Vixseboxse et al. 2021).

In the Flinders Ranges area of South Australia, the Ediacara Member of the Rawnsley Quartzite consists of shallow-marine deposits characterized by well-preserved in situ fossils of the White Sea Assemblage (Gehling 2000). A new unit, the Nilpena Member, characterized by a basal incision, has been informally described and consists of the upper tens of meters of what was previously included in the Ediacara Member (Gehling et al. 2019). Within these two units, taxa of the Ediacara Biota are preserved as casts and molds on the bases of sandstone beds (Gehling 1999). At Nilpena Ediacara National Park (NENP), the excavation and reconstruction of 40 discrete beds, 33 of which preserve at least 10 body fossils, provides approximately 350 m² of Ediacaran seafloor (Fig. 1A). Such an extensive area permits the detailed reconstruction of “snapshots” of Ediacaran communities and provides the opportunity to examine the spatial distributions of constituent populations.

Although seven Ediacaran taxa have been cited as potentially mobile (Evans et al. 2019), the majority of taxa from the Ediacara Member were sessile and lived atop or embedded in laterally extensive microbial mats (Droser et al. 2019, 2022). These mats were abundant in the absence of widespread bioturbation and range

in maturity between beds at NENP (Droser et al. 2022). Among the sessile organisms, the triradialomorph taxa *Tribrachidium* and *Rugoconites* occur in both South Australia and the White Sea of Russia and are abundant at NENP (Glaessner and Daily 1959; Glaessner and Wade 1966; Hall et al. 2015, 2018; Boag et al. 2016). Other sessile taxa, such as the newly described and asymmetrical *Obamus coronatus*, as yet occur only at NENP (Dzaugis et al. 2018).

These three enigmatic taxa have similar diameters and general shapes, but exhibit different bed-to-bed distributions at NENP (Hall et al. 2015, 2018; Dzaugis et al. 2018; Droser et al. 2019). Here we examine the spatial distribution of *Tribrachidium*, *Rugoconites*, and *Obamus* on five excavated beds at NENP through the application of spatial point pattern analysis (SPPA) to determine their spatial distributions and to test hypotheses regarding their life histories, including settlement and dispersal, and potential interactions with their environments. In modern marine invertebrate populations, dispersal mechanisms affect the small- and large-scale spatial distributions of organisms (Wangensteen et al. 2016). Availability of substrate also plays a role during dispersal and settlement, along with preexisting conspecific distributions (e.g., Rodríguez et al. 1993; Sampayo et al. 2020). SPPA takes into consideration common pitfalls in the field of spatial ecology (irregularly shaped study areas, edge effect, etc.) and thus, is ideally suited for Ediacaran surfaces (Wiegand et al. 2006). This study examines small-scale (individual-bed surface distributions) and large-scale data (bed-to-bed distributions) of *Tribrachidium*, *Rugoconites*, and *Obamus* to determine the possible role of dispersal mechanisms and/or environmental factors controlling their distributions.

Geologic Setting and Material.—The Flinders Ranges region of South Australia contains one of the best exposed and most complete successions of Neoproterozoic-aged rocks in the world, including the type section of the Ediacaran Period. Within this succession, the siliclastic, sandstone-dominated Ediacara Member and new informal Nilpena Member of the Rawnsley Quartzite contain an extensive record of

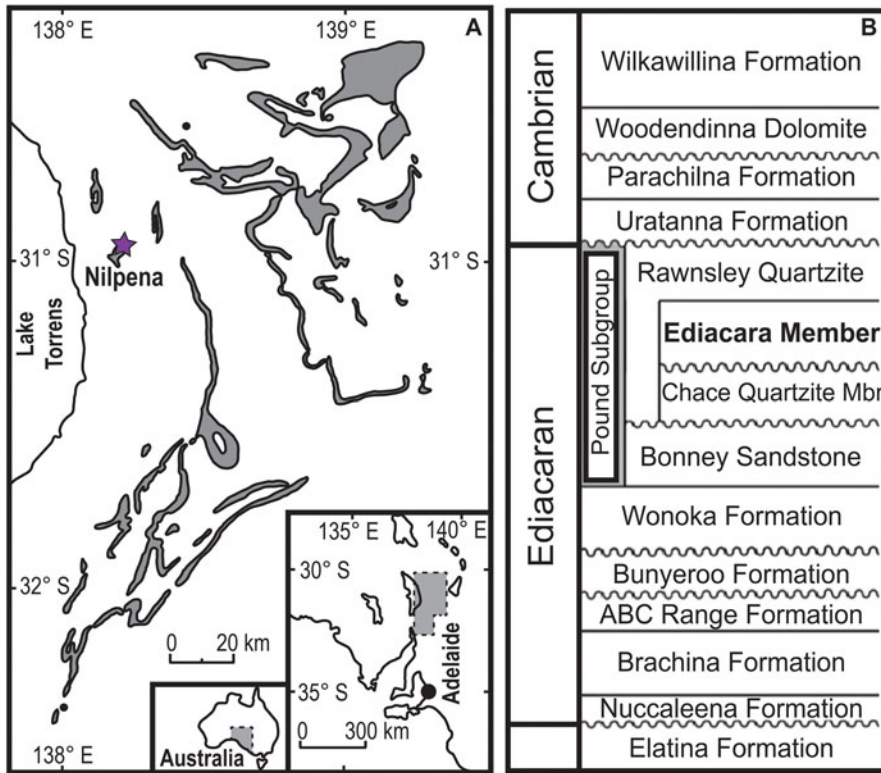


FIGURE 1. A, Distribution of the Pound Subgroup outcrops (gray) bearing the most prominent Ediacaran fossils horizons. Nilpena Ediacara National Park (NENP) is marked by a purple star. B, Stratigraphic locations of the Ediacara Member. Modified from Gehling and Droser (2009).

the Ediacara Biota, cropping out with varying thickness between 10 to 300 m (Gehling 2000; Tarhan et al. 2015a; Droser et al. 2019; Gehling et al. 2019; Fig. 1B). At NENP, west of the Flinders Ranges, a combination of preservation and exposure of the Ediacara and Nilpena Members has uniquely facilitated the excavation and reconstruction of discrete and fossiliferous bedding planes. Their excavation has enabled detailed reconstruction of the ecology, habitat, and fossilization of Ediacaran communities (e.g., Droser et al. 2020; Evans et al. 2020a; Surprenant et al. 2020; Tarhan et al. 2022). Importantly, the shapes and sizes of these beds are a function of geology (e.g., faults), logistics (the beds dip too deeply under the surface), and taphonomy (the bedding surface loses preservational integrity; Hall et al. 2015; Droser et al. 2019). The 33 beds with more than 10 body fossils range in size from 1 to 23 m² and represent, in total, more than 350 m² of Ediacaran seafloor. Numerous beds are excavated from a single pit

and represent continuous stratigraphic successions interbedded with submillimeter- to millimeter-scale beds known as “shims” (Droser et al. 2019).

At NENP, fossiliferous surfaces have been excavated from the Oscillation-Rippled Sandstone Facies (ORS) and the Planar-Laminated and Rip-Up Sandstone Facies (PLRUS; Gehling and Droser 2013; Droser et al. 2017, 2019; Tarhan et al. 2017). The ORS Facies is characterized by submillimeter- to centimeter-thick, rippled, fine- to coarse-grained quartz sandstones interpreted to have been deposited under oscillatory and combined flow between fair-weather- and storm-wave base (Tarhan et al. 2017; Droser et al. 2019). The PLRUS Facies consists of laterally continuous, planar-laminated, fine-grained sandstone beds and is interpreted to have been deposited under unidirectional flow in a sub-wave base upper canyon fill (Gehling and Droser 2013; Droser et al. 2019). Fossils in both facies occur primarily as external

molds on the base of beds. Five beds were used for this study. Bed SE-Rugo, from the ORS Facies, is the only excavated surface within the Ediacara Member with more than 20 specimens of *Rugoconites*. The majority of beds with *Rugoconites* have dispersed populations of fewer than 10 individuals (Table 1). LV-FUN is abundantly populated by *Obamus* and is from the PLRUS Facies. *Tribrachidium* dominates two beds and occurs in an abundance greater than 20 on a third: beds 1T-T and TC-MM3 are from the ORS Facies, while bed WS-TBEW is from the PLRUS Facies. The WS-TBEW bed consists of two non-joining parts, and these are considered separate surfaces for the sake of this study: WS-TBE and WS-TBW.

Tribrachidium is a triradially symmetrical taxon occurring in both the ORS and PLRUS Facies at NENP and the White Sea region of Russia (Glaessner and Daily 1959; Grazhdanin and Ivantsov 1995; Martin et al. 2000; Boag et al. 2016; Ivantsov and Zakrevskaya 2021; Fig. 2A). *Tribrachidium* ranges in size from 0.2 to 4 cm in diameter and occurs in negative hyporelief on the base of 12 surfaces

at NENP, with populations ranging from single individuals on a surface to more than 100 (Hall et al. 2015; Rahman et al. 2015; Droser et al. 2019; Table 1). Both normal and log-normal size–frequency distributions of *Tribrachidium* from NENP suggest that they lived in single-generation populations and reproduced seasonally (Hall et al. 2015). Additionally, *Tribrachidium* has been interpreted as a passive suspension feeder, based on computational fluid dynamics (Rahman et al. 2015). *Tribrachidium* is associated with the fossil form “concentric circles” (Hall et al. 2015; also called concentric ridges or grooves; Glaessner and Wade 1966; Fedonkin 1984). These are interpreted to represent specimens that were flipped before or during episodic burial (preserved as external molds in negative hyporelief) or the cavity left by an organism entirely removed from the seafloor (preserved in positive hyporelief; Fedonkin 1984; Hall et al. 2015). Thus, concentric circles preserved in positive hyporelief are viable for spatial statistical analysis, because they record the presence of a *Tribrachidium*, while negative relief external molds are not viable for spatial statistics, because they

TABLE 1. Adapted from Droser et al. 2019. Beds at Nilpena Ediacara National Park (NENP) on which *Tribrachidium*, *Rugoconites*, and *Obamus* occur. Note that while WS-TBE and WS-TBW are from the same bedding surface, they have been separated here for statistical interpretations. Bold rows indicate beds being examined here.

Bed	Facies	Bed area (m ²)	<i>Tribrachidium</i>		<i>Rugoconites</i>		<i>Obamus</i>	
			Number of individuals	Density (ind/m ²)	Number of individuals	Density (ind/m ²)	Number of individuals	Density (ind/m ²)
1T-T	ORS	4.1	114	27.80	9	2.20	0	0.00
TC-MM3	ORS	17.0	20	1.18	3	0.18	0	0.00
WS-TBE	PLRUS	2.0	24	11.81	0	0.00	0	0.00
WS-TBW	PLRUS	1.7	26	15.16	3	1.75	0	0.00
LV-FUN	PLRUS	22.4	1	0.04	1	0.04	101	4.51
SE-Rugos	ORS	3.6	0	0.00	36	10.00	0	0.00
1T-BOF	ORS	7.3	3	0.41	0	0.00	3	0.41
1T-F	ORS	23.4	9	0.38	6	0.26	0	0.00
1T-LS	ORS	1.4	1	0.71	0	0.00	0	0.00
1T-NA	ORS	4.1	0	0.00	10	2.44	6	1.46
STC-AB	ORS	3.4	1	0.29	0	0.00	0	0.00
STC-B	ORS	10.8	0	0.00	3	0.28	0	0.00
STC-F	ORS	12.9	0	0.00	2	0.16	0	0.00
STC-G	ORS	13.2	0	0.00	2	0.15	0	0.00
STC-I	ORS	15.4	0	0.00	7	0.45	0	0.00
STC-J	ORS	11.9	0	0.00	10	0.84	0	0.00
STC-X	ORS	9.0	3	0.33	0	0.00	0	0.00
TB-ARB	ORS	13.1	0	0.00	0	0.00	10	0.77
WS-MAB	PLRUS	3.3	2	0.61	0	0.00	0	0.00
WS-SUB	PLRUS	3.9	6	1.54	0	0.00	0	0.00

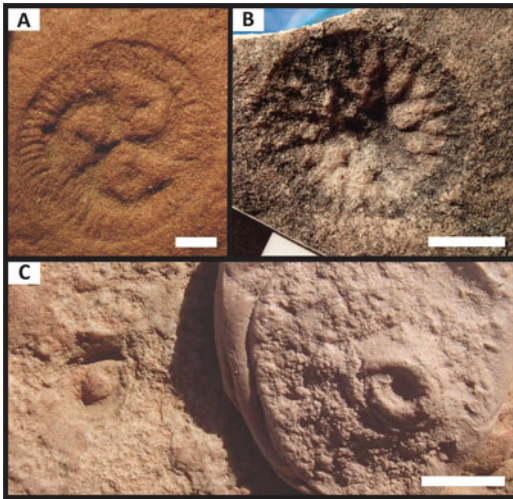


FIGURE 2. A, *Tribrachidium*, a triradial taxon found at Nilpena Ediacara National Park (NENP) and the White Sea of Russia. B, *Rugoconites*, another triradial taxon found in Australia and the White Sea. C, *Obamus*, a torus-shaped taxon found only at NENP. As it was deeply embedded in the microbial mat a Silly Putty mold (right) was placed next to the individual to show what the organism would have looked like on the seafloor. Scale bars, 1 cm.

record a transported specimen. Previous nearest-neighbor analyses suggested that one population of *Tribrachidium* at NENP was distributed randomly (Bed 1T-T; Hall et al. 2015).

Rugoconites is another triradial taxon that occurs in Australia and Russia, with a single poorly preserved possible specimen reported from Canada (Glaessner and Wade 1966; Narbonne and Hofmann 1987; Hall et al. 2015, 2018; Fig 2B). *Rugoconites* is generally circular and has a size range of 1 to 6 cm in diameter (Glaessner and Wade 1966; Hall et al. 2015, 2018). Specimens occur in negative hyporelief on the base of 14 surfaces at NENP in both the PLRUS and ORS Facies, with the majority of populations consisting of fewer than 10 individuals (Table 1). The size–frequency distributions of *Rugoconites* suggest that, similar to *Tribrachidium*, populations were composed of single generations or cohorts (Hall et al. 2018). As with *Tribrachidium*, analyses were run on both normal and log-normal body-size diameters, with the same results for each (Hall et al. 2018). Both *Tribrachidium* and *Rugoconites* have been interpreted to be environmental generalists, based on their wide environmental

distributions and association with both mature and immature microbial mats and a variety of other taxa (Grazhdankin and Ivanstov 1995; Hall et al. 2015, 2018; Droser et al. 2019).

Obamus is a torus-shaped organism that lived embedded in the microbial mat that covered the Ediacaran seafloor. It is preserved in negative hyporelief (Dzaugis et al. 2018; Fig 2C). Specimens of *Obamus* have been identified on four surfaces from both the ORS and PLRUS Facies (Table 1). Previous studies have noted that *Obamus* appears to be common in areas of mature organic mats (Dzaugis et al. 2018; Droser et al. 2022). Unlike *Tribrachidium* and *Rugoconites*, which both occur on multiple continents with significant paleogeographic separation (Grazhdankin and Ivanstov 1995; Hall et al. 2015, 2018; Droser et al. 2019), *Obamus* has thus far only been found at NENP and only in association with mature microbial mats.

Spatial Distributions.—The spatial distribution of sessile organisms can be used to test hypotheses about reproductive strategies, competition, and environmental impacts (Kenkel 1988; Harms et al. 2000; He and Legendre 2002; Atkinson et al. 2007; Jacquemyn et al. 2007; Watson et al. 2007; Wiegand et al. 2007a; Law et al. 2009; Franklin and Santos 2010; Zillio and He 2010; Lin et al. 2011; Schleicher et al. 2011; Chang and Marshall 2016; Carrer et al. 2018; Mitchell and Harris 2020). Distributions can be described as either aggregated, random, or segregated (Fig. 3). In both terrestrial and marine ecosystems, aggregation (also described as clustering or clumping) is by far the most common distribution, often resulting from dispersal limitations and/or environmental controls (Carlson and Olson 1993; Karlson et al. 1996; He and Legendre 2002; Franklin and Santos 2010; Lin et al. 2011; Carrer et al. 2018; Lesneski et al. 2019; Ben-Said 2021; Fig. 3A). Mathematically, an aggregated pattern is one in which the neighborhood density (the number of points separated by a distance) is high enough that points tend to be located nearer to each other than expected based on a random null model (Wiegand and Moloney 2014). For example, strongly aggregated patterns of sexually reproducing marine benthic invertebrates can be the result of habitat-selective larval stages, short-

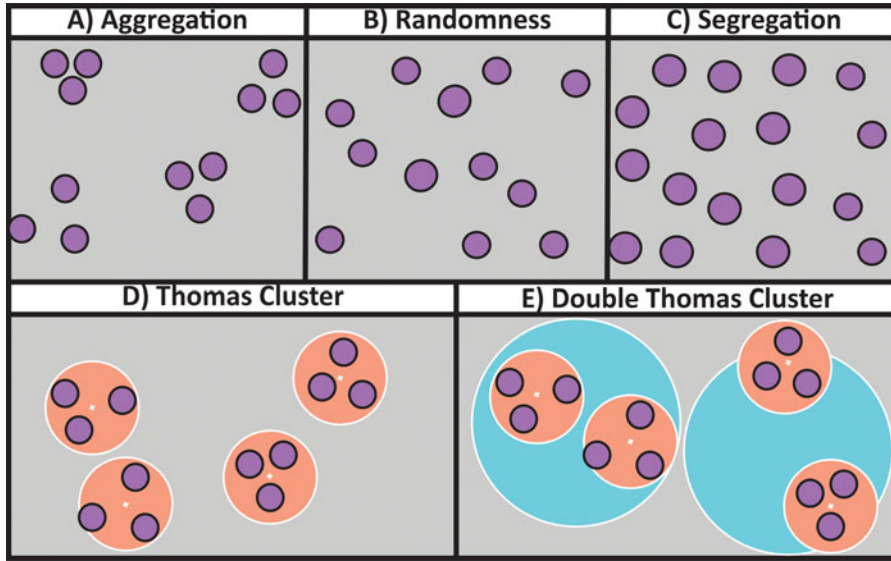


FIGURE 3. Common types of spatial distributions found in modern ecosystems. Small purple dots indicate the locations of individuals of a certain taxon. A, Aggregation: individuals being closer together than would be predicted in a random distribution. B, Randomness: individuals are in a Poisson distribution. C, Segregation: points are farther apart than predicted in a random distribution, resulting in a uniform pattern. D, Thomas cluster (medium orange circles): individuals are aggregated around a center point at varying distances. E, Double Thomas cluster (large blue circles): a nested cluster pattern in which two sets of clusters are present at two spatial scales.

lived/dispersed larval stages, and/or a preference for being near conspecifics (Carlson and Olson 1993).

Random patterns are less common in modern ecosystems but have been associated with certain marine organisms as a function of settlement (Schmidt 1982; Guy-Haim et al. 2015; Fig. 3B). For example, the southern Californian bryozoan *Bugula neritina* has random distributions due to larvae not having a preference for substrate or being near a conspecific (Keough 1984). At the ecosystem scale, a random pattern has been interpreted to represent a community whose distribution is not controlled by biological (dispersal limitations, settlement preference, etc.) or environmental constraints (limited resource, widely dispersed patches, etc.; Davis and Campbell 1996; Brenchley and Harper 1998). Mathematically, random distributions are Poisson processes wherein points are randomly and independently located within an area (Wiegand and Moloney 2014; Velázquez et al. 2016; Ben-Said 2021).

Organisms can also be segregated (also known as regular, uniform, or hyperdispersed) and, like aggregation, segregation is

determined through comparison with the null model of a random distribution (Ben-Said 2021). Mathematically, this pattern occurs when the neighborhood density is lower than a random pattern, resulting in points that are regularly spread out (Wiegand and Moloney 2014; Fig. 3C). Ecologically, this distribution is associated with competition, specifically intra-specific competition, as individuals will maintain a certain distance apart to ensure resource acquisition occurs without competition, or habitat association, where the underlying habitat is segregated (Kenkel 1988; Brenchley and Harper 1998; Lin et al. 2011; Mitchell and Kenchington 2018). Additionally, segregation can be a result of habitat patchiness (Mitchell and Kenchington 2018). For example, the modern South Australian ascidian *Clavelina moluccensis* has been noted to settle in a segregated (regular) pattern as a result of interspecific competition (Davis and Campbell 1996).

The bed-scale spatial distributions of *Rugocornites* and *Obamus* have not previously been examined, and only one population of *Tribrachidium* at NENP has been analyzed for spatial distribution (1T-T = random distribution via

nearest-neighbor analysis; Hall et al. 2015). Using SPPA instead of nearest-neighbor analysis allows greater spatial scales to be covered. Here we examine the spatial patterns of these benthic sessile taxa on six different surfaces in order to test possible biological and ecological controls on their distributions and gain insight into their reproductive and dispersal methods.

Methods

Spatial distributions of *Tribrachidium*, *Rugocnites*, and *Obamus* were analyzed from six surfaces at NENP. Surfaces were logged and mapped using a centimeter-scale grid (Fig. 4, Supplementary Fig. 1) (for more information on bed mapping, see Droser et al. [2019]). To control for possible variations in preservation potential across each surface, each bed was examined on the centimeter scale for variations in preservation of textured organic surfaces (mats). If there were preservational gaps in the mat and/or the surface was fretted, we digitally removed that area. Specifically, we only included areas of the bed in which both the mat texture and the organism are clearly preserved and in situ. Using this approach, fretted portions of both TC-MM3 (original area = 21.56 m²; edited area = 17 m²) and 1T-T (original area = 4.4 m²; edited area = 4.1 m²) were digitally excluded.

To capture both the irregular shapes and edges of the surfaces, hundreds of photographs were taken and compiled in the photogrammetric 3D modeling software Agisoft Metashape (field methods adapted from Mallison and Wings [2014]). The borders of the surfaces were then drawn out in ArcGIS to create borders accurate to the millimeter-scale in which the taxa coordinates are plotted. Because the shapes, sizes, and population densities of taxa are out of excavators' control, excavated surfaces at NENP act as "random" samples of Ediacaran ecosystems.

The six surfaces were chosen based on the number of individual *Tribrachidium*, *Rugocnites*, or *Obamus* present on each surface, with a minimum requirement of 20 individuals per surface (Table 1). Concentric circles preserved in positive relief on WS-TBE and WS-TBW were included in combination with classically preserved *Tribrachidium*, as they represent the

locations of specimens "pulled out" before burial, presumably by a storm (Hall et al. 2015). Negative hyporelief concentric circles on 1T-T were not used, because they are interpreted as non-in situ *Tribrachidium* that have been pulled out; however, the few positive concentric circles on that surface were used (Hall et al. 2015).

Bed-to-bed distributions of taxa were determined using data published by Droser et al. (2019) on density (number of individuals/square meters) and abundance within each of the two facies and excavation sites (Table 1). Bed surface-scale spatial distributions of each taxon were tested against a random pattern to identify aggregation, segregation, or a lack thereof via SPPA in Programita and the R package Spatstat (Wiegand and Moloney 2014; Baddeley et al. 2016). Previous studies have used SPPA to investigate the distributions of the Ediacara Biota (Mitchell et al. 2015, 2018, 2020; Coutts et al. 2018; Mitchell and Butterfield 2018; Mitchell and Kenchington 2018). The work presented here is the first use of SPPA to interpret *Tribrachidium*, *Rugocnites*, and *Obamus* distributions.

SPPA is divided into three major statistical components that allow for biological and ecological characteristics to be interpreted.

Summary Statistics.—Summary statistics quantify the properties of an observed pattern using functions of distance. Multiple summary statistics are required for a complete analysis (Franklin and Santos 2010; Wiegand and Moloney 2014). Summary statistics can be divided into two categories: first-order summary statistics, or those which examine the configuration of individual points; and second-order summary statistics, which are based on the spatial relationships of pairs of points (Wiegand and Moloney 2014). The main summary statistic used here is the pair-correlation function (PCF), which is a second-order summary statistic that calculates the pairwise distance from each point to each other point, and then establishes how many points are found within a given radius (r) from the average/typical point (Illian et al. 2008; Wiegand and Moloney 2014; Velázquez et al. 2016). PCF will continue to examine pairs at different distances until the range of correlation (r_{corr}) is reached. The range of correlation is the distance at which PCF is no

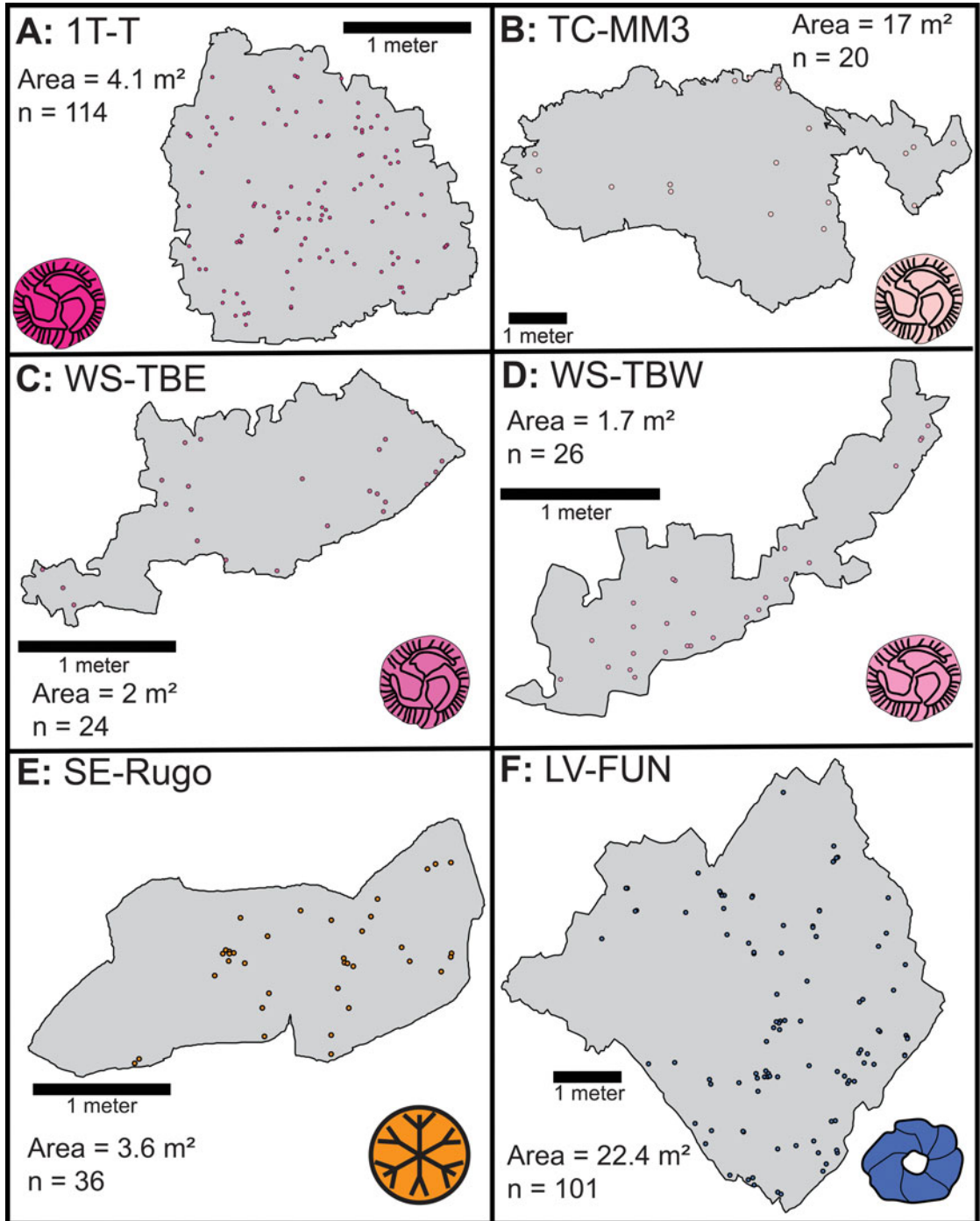


FIGURE 4. Excavated surfaces examined in this paper. This figure only shows *Tribrachidium*, *Rugoconites*, and *Obamus* locations on their respective beds. Other taxa were left out for the convenience of the reader. Dots are not to scale. Note that surfaces WS-TBE and WS-TBW are from the same bed, but were unable to be attached during excavation. As such, they are treated as two separate surfaces here. Additionally, locations on TC-MM3 with poor preservation were removed to account for taphonomic heterogeneity. A–D, *Tribrachidium* populations are plotted in different shades of pink. E, *Rugoconites* populations are plotted in orange. F, *Obamus* populations are plotted in blue.

longer statistically relevant due to the shape and size of the study area, and typically is half the width of the thinnest part of the study area (Illian et al. 2008; Baddeley et al. 2016). The L-function (LF) was also used to examine the distributions on selected surfaces. This method examines the number of points within a circle whose radius is r , and will continue to increase in size till the r_{corr} is reached. The LF was used to support PCF results, and LF plots are provided in Supplementary Figures 2–4.

Null Models.—Both the LF and PCF were used in tandem with null models—patterns that represent a null hypothesis or standards to which an observed population’s distribution is compared (Wiegand and Moloney 2014; Velázquez et al. 2016). Null models are based on the number of points within a study area and their reorientation into common spatial patterns (e.g., a random pattern; Wiegand and Moloney 2014; Velázquez et al. 2016). For the work presented here, each null model was run through 999 Monte Carlo simulations. The highest and lowest 49 Monte Carlo simulation values were taken to create a simulation envelope (see “Confidence Tests”). We chose 999 Monte Carlo simulations because the higher number of simulations used will increase the accuracy of the simulation envelope (Velázquez et al. 2016) and 999 is considered large without being too computationally taxing (Wiegand and Moloney 2014). The highest and lowest 49 values were chosen, as they are the upper and lower 5% of the simulated data and result in a probability error of 0.05 as recommended by Illian et al. (2008). The summary statistic line was then plotted over the simulation envelope, revealing the spatial scales at which a positive (above the simulation envelope), negative (below the simulation envelope), or neutral (within the simulation envelope) relationship is present.

In these plots the x-axis represents the radius from the center of each specimen and the y-axis is the summary statistical function value. The higher the function value, the stronger the spatial pattern, and vice versa (Dhungana and Mitchell 2021). The first (and primary) null model tested was complete spatial randomness (CSR), also known as the homogenous Poisson null model, which determines if a pattern is

random, aggregated, or segregated. While the CSR null model is suitable for determining the gross spatial distribution of organisms, it is best used in tandem with other models, such as the heterogenous Poisson (HP) null model, to determine the most likely underlying process behind nonrandom patterns (Wiegand and Moloney 2014). The HP null model determines whether a pattern is random (i.e., points are independently distributed) while allowing the intensity (density) of points in an area to vary depending on location (Wiegand et al. 2007a; Schleicher et al. 2011; Wiegand and Moloney 2014; Velázquez et al. 2016; Carrer et al. 2018). As this method accounts for varying densities, the HP null model has been used to identify environmental heterogeneities in an ecosystem (soil nutrients, topography, etc.; Wiegand et al. 2007a; Wiegand and Moloney 2014; Velázquez et al. 2016; Carrer et al. 2018). Thus, the HP model assesses whether the observed patterns are the same, more aggregated, or more segregated than the null model, whereas the CSR model is the only model that determines absolute randomness, aggregation, and segregation.

If a population was determined to be aggregated, we also tested for a Thomas cluster (TC) and double Thomas cluster (DTC), aggregation patterns common in modern taxa (Wiegand et al. 2007b). The TC null model determines whether individuals are aggregated around a center point at varying distances with randomly distributed cluster centers (Wiegand et al. 2009; Wiegand and Moloney 2014; Fig. 3D). The TC can be further analyzed to determine whether the pattern fits a nested cluster, more commonly known as DTC (Fig. 3E). In this model, smaller TCs are located within the larger DTC, and cluster centers are not random (Wiegand et al. 2009). Determining whether organism distributions fit a TC and DTC has been used to investigate the dispersal of offspring in a given area for both modern and fossilized ecosystems (Wiegand et al. 2009; Mitchell et al. 2015; Mitchell and Harris 2020; Dhungana and Mitchell 2021). While the TC and DTC null models are sometimes referred to as the CSR+TC and CSR+DTC null models, we choose to refer to them as the former, which are more consistent

with current literature (e.g., Mitchell et al. 2020; Dhungana and Mitchell 2021).

Finally, to rule out environmental heterogeneity as a driver of distribution patterns among *Tribrachidium*, *Rugoconites*, and *Obamus*, populations were tested against a heterogenous Poisson Thomas cluster (HPTC) and heterogenous Poisson double Thomas cluster (HPDTC). These methods were used to determine whether any form of heterogeneity, and specifically environmental heterogeneity, was present. Similar to the manner in which TC and DTC determine whether a surface has individuals aggregated around a center point (TC) or whether those clusters are nested (DTC), the HPTC and HPDTC methods determine whether the population fits those patterns while also considering how the intensity of the pattern varies depending on the locations of the points within the study area. It is important to note that nested clusters can also occur when you have TC on a background HP aggregation, so it is prudent to test for DTC versus HPTC to determine whether there are multiple reproductive events or a single reproductive event with environmental filtering.

Confidence Tests.—To determine whether certain patterns fit a specific null model, the analytical global envelope (AGE) was used, and are depicted as the colored simulation envelopes in our results (shades of pink = *Tribrachidium*, orange = *Rugoconites*, blue = *Obamus*). The AGE was chosen because it incorporates information on the number of individuals, the size and shape of the fossil surfaces, other aspects of the summary statistics lost during a pointwise simulation envelope (indicated as the black dotted line within the colored simulation envelope) and is the more popular method (Wiegand et al. 2016). It is important to note that the more points (in this case, fossils) included in a test, the thinner the AGE will be.

We also used goodness-of-fit (GoF; referred to as “pd” in text) tests to determine whether taxon patterns matched any of the null models. The GoF is similar to a *p*-value: a value of 0.0 indicating a complete rejection of the specific null model, while 1.0 indicates a perfect fit (Mitchell et al. 2020). It is vital to note that GoF tests are only used in an auxiliary fashion and cannot override a visual inspection of the AGE and

summary statistic plot (Wiegand and Moloney 2014).

Three rounds of smoothing were done on each surface for each summary statistic and null model tested in order to smooth out the noise inherent in all signals (Mitchell et al. 2019). Smoothing was conducted in Programita by increasing the ring width, or the size of the area examined by PCF, and centered around a typical point, from which the expected density of the points (in this case individual fossils) is determined (Wiegand and Moloney 2014). The initial ring width size was determined by Programita and smoothed by increasing ring width size by odd-numbered intervals as was suggested in Wiegand and Moloney (2004) and Wiegand and Moloney (2014). The suggested and chosen ring width values are presented in Supplemental Table 1.

Results

Tribrachidium.—SPPA results show that 1T-T *Tribrachidium* are aggregated (Figs. 5A, 6A). Both the TC and DTC models provide good fit to the observed pattern, with DTC as the best fit (best-fit pd = 0.573) (Fig. 7A,D, Table 2). The initial aggregation value for CSR null models has a PCF value of 2.84. None of the heterogeneous null models (HP, HPTC, or HPDTC) were a good fit for the 1T-T *Tribrachidium* population. *Tribrachidium* populations on TC-MM3, WS-TBE, and WS-TBW best fit an HP null model, indicating that while their gross distributions might be considered aggregated (when tested against the CSR null model), when taking spatial heterogeneity into account, the *Tribrachidium* are better described by a random distribution, albite one that is restricted (TC-MM3 best-fit pd = 0.157; WS-TBE best-fit pd = 0.555; WS-TBW best-fit pd = 0.932) (Fig. 6B–D, Table 2).

Rugoconites.—The population of *Rugoconites* on SE-Rugo is aggregated (Figs. 5E, 6E). Both a TC and a DTC provide good fit to the observed pattern, with DTC as the best fit (best-fit pd = 0.797) (Fig. 7B,D, Table 2). The heterogeneous models (HP, HPTC, or HPDTC) were not good fits for the *Rugoconites* population on SE-Rugo.

Obamus.—On LV-FUN, *Obamus* are strongly aggregated and have good fit to both TC and DTC models, with the TC null model as the

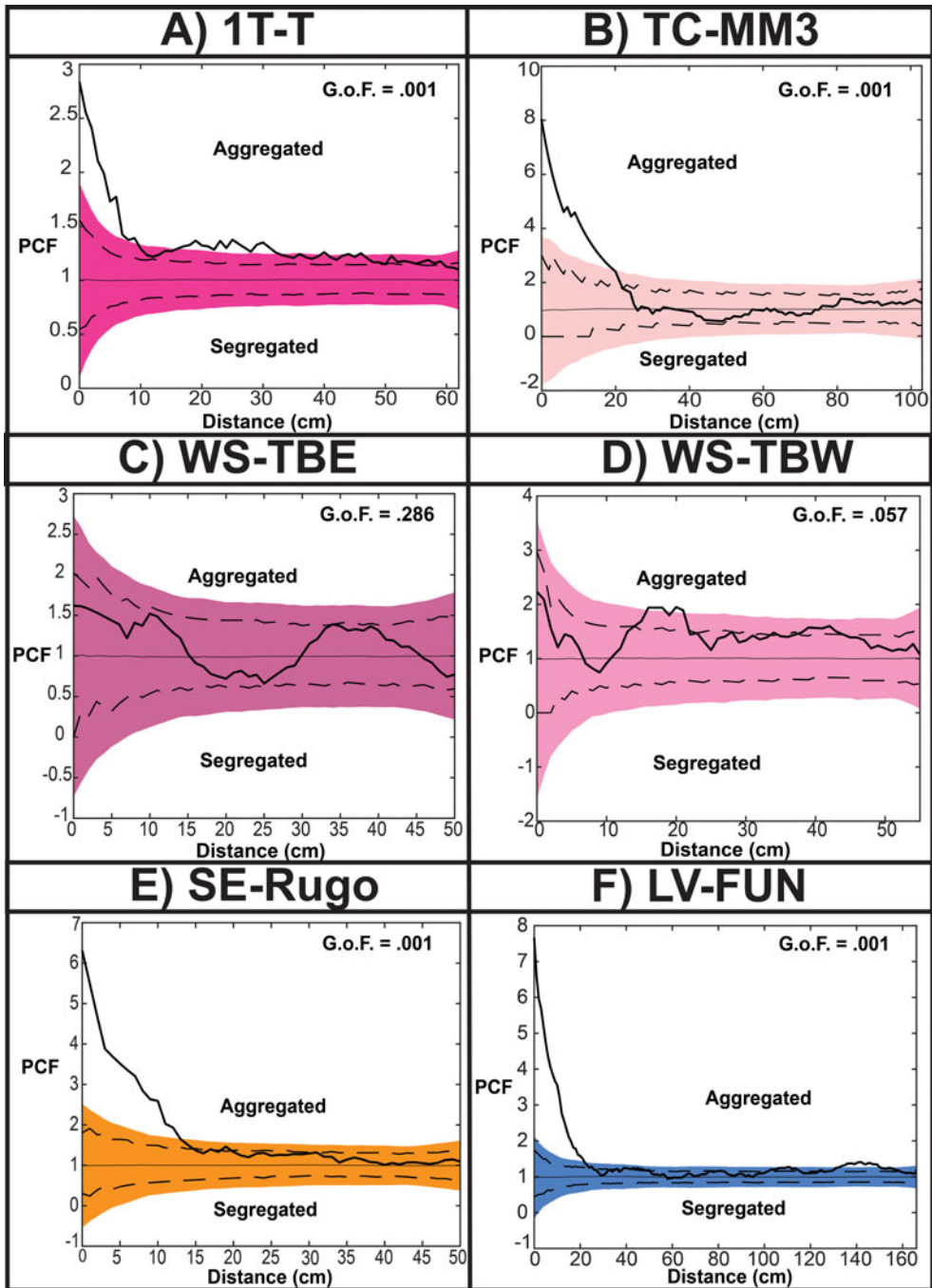


FIGURE 5. Complete spatial randomness (CSR) results for the beds examined. Colored simulation envelopes are analytical global envelopes (AGE), dotted lines are pointwise simulation envelopes, thick black line is summary statistic value. A,B, *Tribrachidium* on 1T-T and TC-MM3 show aggregation at short scales. C, *Tribrachidium* on WS-TBE are spatially random. D, *Tribrachidium* on WS-TBW are aggregating from 15 to 22 cm. E,F, *Rugoconites* on SE-Rugo and *Obamus* on LV-FUN both display aggregated distributions. GoF, goodness-of-fit.

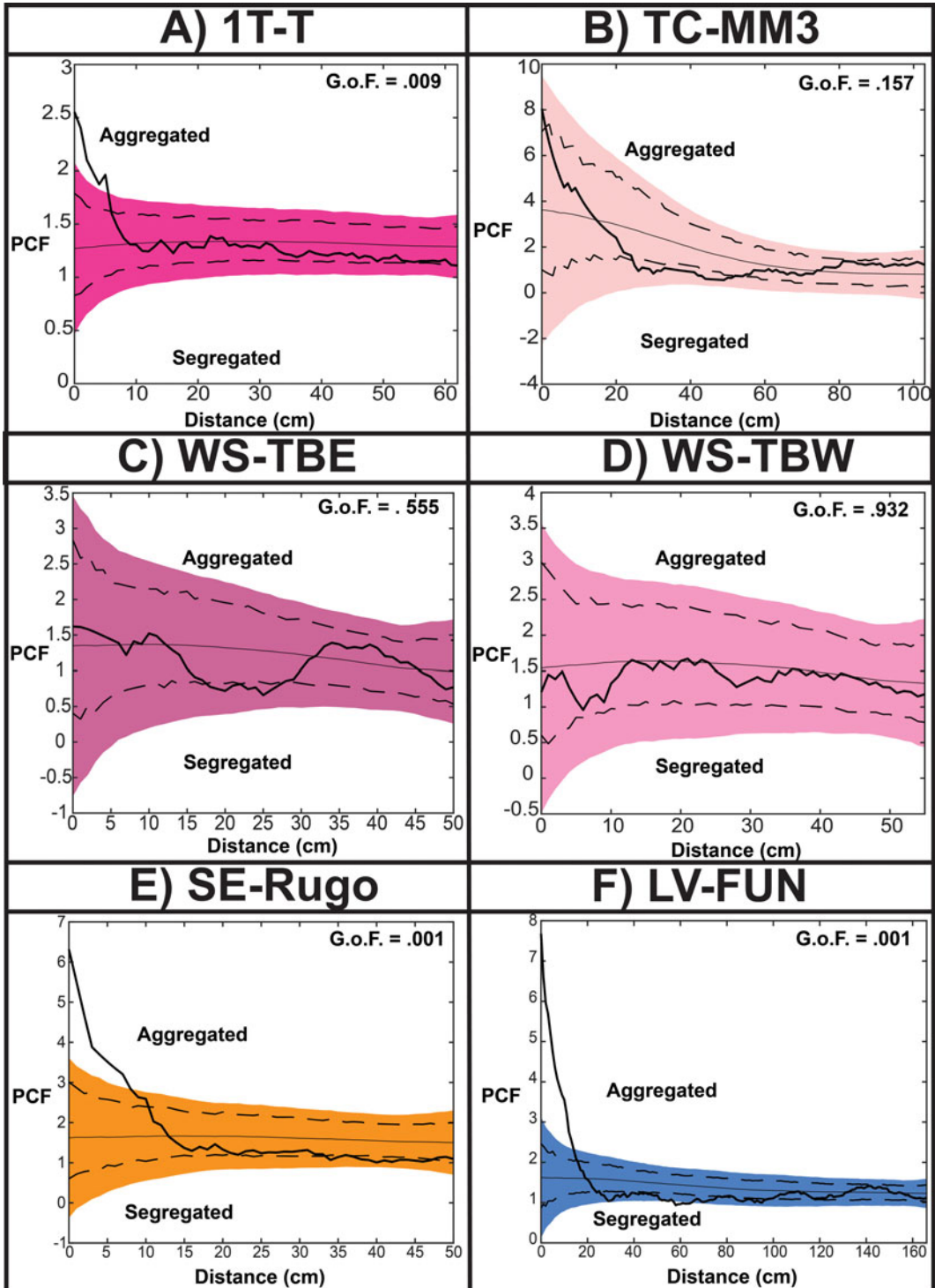


FIGURE 6. Heterogeneous Poisson (HP) results for the beds examined. Colored simulation envelopes are analytical global envelopes (AGE), dotted lines are pointwise simulation envelopes, thick black line is summary statistic value. A, *Tribrachidium* on 1T-T does not fit the HP null model, while those on B–D TC-MM3, WS-TBE, and WS-TBW were best fit to the HP null model, implying spatial heterogeneity. E, F, *Rugocnites* on SE-Rugo and *Obamus* on LV-FUN both do not fit the HP null model. GoF, goodness-of-fit.

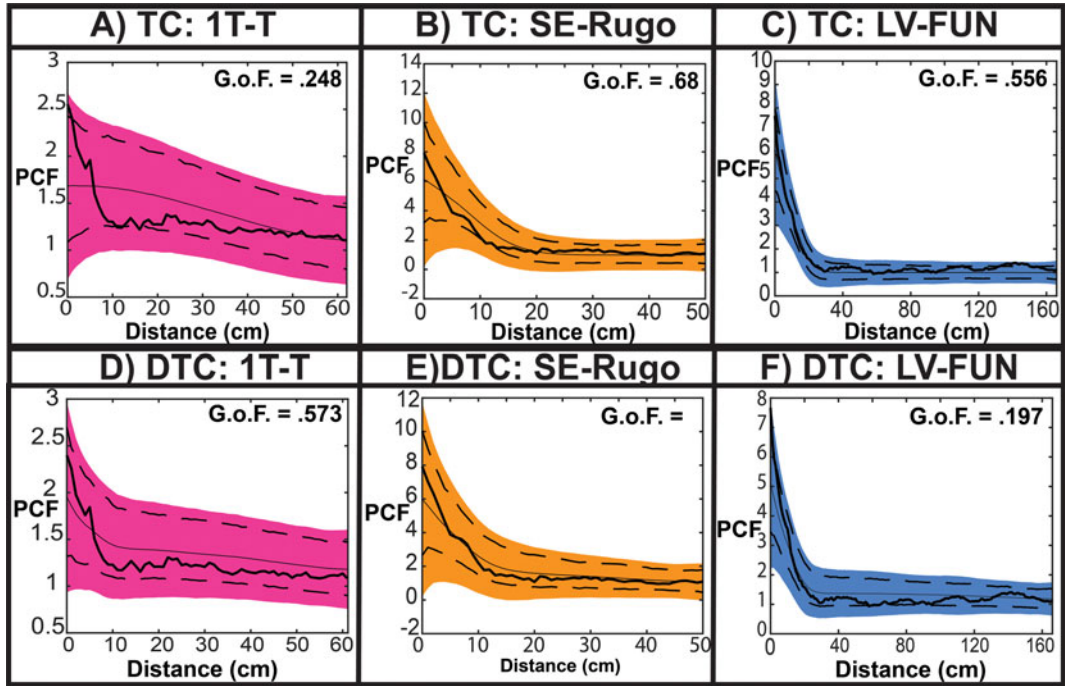


FIGURE 7. Thomas cluster (TC) and double Thomas cluster (DTC) null model results. Colored simulation envelopes are analytical global envelopes (AGE), dotted lines are pointwise simulation envelopes, thick black line is summary statistic value. Note that only communities that were aggregated could be tested against a TC or DTC null model. A–F, All three of the aggregated populations were fit to both a TC and DTC. GoF, goodness-of-fit.

best fit (best-fit $pd = 0.556$) (Figs. 5F, 6F, 7C,F, Table 2). Strong aggregation was determined by examining the initial aggregation values calculated using a CSR null model, revealing a

PCF value of 7.66, significantly outside the AGE (Fig. 5F). The heterogenous models (HP, HPTC, or HPDTC) were not good fits for the *Obamus* population on LV-FUN.

TABLE 2. Parameters and goodness-of-fit (GoF) results for the various null models examined here. A GoF = 1 is a perfect fit to the null model being tested, while GoF = 0 is a rejection. All beds were tested against the complete spatial randomness (CSR) and heterogenous Poisson (HP) null models. If aggregated, they were additionally tested against Thomas cluster (TC) and double Thomas cluster (DTC) null models. The number of estimated clusters and their sizes has been included here. Finally, all surfaces were tested against heterogenous Poisson Thomas cluster (HPTC) and heterogenous Poisson double Thomas cluster (HPDTC) null models to additionally test for environmental heterogeneity. PCF, pair-correlation function. Bolded values indicate which null model was the best fit to the population.

Bed	<i>n</i>	Area	Density	r_{corr}	GoF values for PCF (1.0 = perfect fit, 0.0 = rejection)						Cluster sizes		Number of clusters	
					CSR	HP	TC	DTC	HPTC	HPDTC	TC	DTC	TC	DTC
1T-T	114	4.1	27.8	62	0.001	0.009	0.248	0.573	0.038	0.038	34.31	15.7 (L), 518.8(S)	17.44	0.037(L), 1.22 (S)
TC-MM3	20	18.2	1.1	103	0.001	0.157	N/A	N/A	0.1538	0.067	N/A	N/A	N/A	N/A
WS-TBE	24	2.0	11.8	50	0.284	0.555	N/A	N/A	0.119	0.09	N/A	N/A	N/A	N/A
WS-TBW	26	1.7	15.2	55	0.057	0.932	N/A	N/A	0.102	0.029	N/A	N/A	N/A	N/A
SE-Rugo	36	3.6	10.0	50	0.001	0.001	0.68	0.797	0.108	0.136	10.93	30.9 (L), 7.1 (S)	18.66	17.9 (L), 43.2 (S)
LV-FUN	101	22.4	4.5	101	0.001	0.001	0.556	0.197	0.027	0.05	11.85	184.6 (L), 11.5 (S)	73.05	8.7 (L), 107.4 (S)

Discussion

Each taxon examined here, and specifically *Tribrachidium*, displays different population densities and distributions across the surfaces at NENP (Table 1). *Tribrachidium* has varying distributions throughout NENP, ranging from isolated individuals, to random distributions on multiple heterogeneous surfaces, to an aggregated single-generation population on surface 1T-T. Varying spatial distribution patterns have been documented among both modern organisms (e.g., the European barnacle *Chthamalus stellatus* has both random and aggregated patterns; Guy-Haim et al. 2015), and Ediacaran taxa (e.g., *Aspidella* specimens from three surfaces excavated from both the Olenek Uplift and the White Sea; Mitchell et al. 2020).

The aggregated distribution contrasts with previous spatial analytical results yielding random distributions for *Tribrachidium* on 1T-T (Hall et al. 2015). This disparity is a function of the application of different methods; Hall et al. (2015) used nearest-neighbor analysis, which as they note was hampered by irregularly shaped study areas and edge effects. Additionally, nearest-neighbor analysis is limited to the largest nearest-neighbor distance, so it can normally only handle scales much smaller than spatial scales captured by PCF. The aggregated distribution of *Tribrachidium* on 1T-T is an outlier compared with the other *Tribrachidium* surfaces examined here. It is not uncommon for generally solitary and/or randomly distributed marine sessile invertebrates to be densely populated if advantageous environmental conditions permit (Schmidt 1982; Rossi and Snyder 2001); however, the specific settlement conditions that enabled *Tribrachidium* to be very abundant and dense on 1T-T (density = 28 individuals/m²) are unknown. Both settlement conditions or post-settlement environmental filtering could allow for strong aggregation, and it is not possible to distinguish between the two with the methods used here. *Tribrachidium* on TC-MM3, WS-TBE, and WS-TBW are best fit to an HP null model, implying the presence of an external effect, such as environmental heterogeneity, on their distribution. The cause of this heterogeneity is unknown, but did not impact the settlement

or life span of the 1T-T *Tribrachidium* population. It could be that there were originally dense populations of *Tribrachidium* on TC-MM3, WS-TBE, and WS-TBW but that organisms died over time as a result of post-settlement filtering.

At NENP, *Tribrachidium* is found on 12 surfaces (from two facies) exhibiting variable community development, diversity, paleobathymetry, and microbial mat maturity. *Tribrachidium* has been found as solitary individuals on three of those surfaces (STC-AB, 1T-LS, LV-FUN; Table 1), implying that the aggregation found on 1T-T is not likely a function of *Tribrachidium* being spatially limited in its dispersal or requiring conspecifics nearby for reproductive purposes, as is the case for some modern invertebrates (Pawlik 1992; Rodríguez et al. 1993; Davis and Campbell 1996). Reproductive method can play a role in the dispersal of an organism even if said organism does not need to be near conspecifics for post-settlement reproduction. While it is possible that *Tribrachidium* had multiple modes of reproduction resulting in different dispersal patterns, previous work determined that they likely had a seasonal or opportunistic sexual reproductive method, with clear size cohorts on NENP surfaces (Hall et al. 2015). Similarly, Zakrevskaya (2014) found a single size cohort of *Tribrachidium* at a White Sea locality. Among modern marine invertebrates, there is a positive relationship between the supply of larvae and settlement rates that operates over multiple spatial scales (0–100 m, 100–1000 m, and 100–1000 km; Jenkins 2005). An organism reproducing via opportunistic sexual reproduction could secure a substrate with a preexisting low species diversity and populate the surface with high abundance. This method of dispersal could be detected as aggregation, as it is a function of increased density, due to the nature of SPPA. If more points are added to a “study area,” then it is more likely that the average neighborhood density (i.e., the number of points separated by a distance [r]) will have a higher value than that of a random distribution, thus resulting in an aggregated pattern (Wiegand and Moloney 2014). The combination of weak aggregation and higher density compared with *Rugosconites* or *Obamus* (1T-T: 28 individuals/m²;

SE-Rugo: 10 individuals/m²; LV-FUN: 5 individuals/m²), supports the hypothesis that the distribution of *Tribrachidium* on 1T-T is likely a function of preferred settlement conditions or low post-settlement environmental filtering (Table 1).

The fact that different populations of *Tribrachidium* exhibit various spatial distributions and densities may also further support that *Tribrachidium* was able to live and thrive in a wide variety of environmental and ecological settings. While the process leading to the densely populated and aggregated distribution of *Tribrachidium* on 1T-T is unknown, an opportunistic life strategy could secure a substrate with high availability in ecospace (Hall et al. 2015).

These results may also have implications for our understanding of other ecological aspects of *Tribrachidium*. Using computational fluid dynamics, Rahman et al. (2015) found that modeled fluid flow around a *Tribrachidium* supported the conclusion that *Tribrachidium* was a passive suspension feeder, but their simulations only modeled flow around a single *Tribrachidium* fossil. The authors suggest that a dense community would have helped enable a consistent flow of suspended nutrients. A similar study that modeled fluid flow around aggregated *Ernietta* fossils found that a gregarious lifestyle would have aided suspension feeding for those organisms (Gibson et al. 2019), which could similarly hold for *Tribrachidium*, despite differences in morphology. Based on an observational study of *Tribrachidium* morphology, Ivantsov and Zakrevskaya (2021) instead proposed that *Tribrachidium* fed using a more active feeding style, moving food particles along branched grooves, interpreted based on the “frill” commonly preserved on White Sea specimens. Modeling fluid flow around aggregated and randomly distributed *Tribrachidium* may help constrain whether their presumed feeding style also played a role in their spatial distributions, or whether certain feeding styles can be ruled out based on the existence of both aggregated and randomly distributed populations.

As previously noted, *Rugoconites* occurs on multiple surfaces with differing diversity, facies, and microbial mat maturity (Hall et al. 2018). *Rugoconites* occurs as low abundance

and density populations on 11 beds at NENP (Table 1). *Rugoconites* on SE-Rugo was best fit to a DTC model, suggesting that these organisms were distributed in clusters of clusters (best-fit $pd = 0.797$) (Fig. 7B,E). Aggregation, in a general ecological sense, implies that either a biological or environmental factor is affecting the distribution of an organism (Carlson and Olson 1993; Karlson et al. 1996; He and Legendre 2002; Franklin and Santos 2010; Lin et al. 2011; Ambroso et al. 2013; Carrer et al. 2018). The intensity of aggregation detected on SE-Rugo is stronger than on 1T-T’s *Tribrachidium* population (initial PCF values for 1T-T: 2.84; SE-Rugo: 6.32) (Fig. 5A,E); however, the population density of *Rugoconites* is still high compared with other taxa at Nilpena (Droser et al. 2019; Table 1). This high density implies that while the aggregation is not solely a function of density-dependent processes, *Rugoconites* is possibly another example of an opportunistic or seasonally reproducing organism having advantageous settlement conditions or low post-settlement mortality rates. Hall et al. (2018), using size–frequency distributions from surfaces including SE-Rugo, determined that *Rugoconites* at NENP likely reproduced sexually.

Benthic marine invertebrates that reproduce sexually can exhibit strong aggregation related to dispersal and/or settlement mechanisms. Specifically, three methods result in strong aggregation: habitat-selective larval stages, short-lived/dispersed larval stages, and/or a preference for being near conspecifics (Carlson and Olson 1993; Lesneski et al. 2019). While *Rugoconites* is more common in the ORS Facies, it is found in numerous environments with no apparent preference for substrate, suggesting that a selective larval stage is unlikely. Most benthic invertebrates need to be near a conspecific to reproduce sexually, whether the distance is centimeters, millimeters, or kilometers in scale, although, there are taxa with reproductive ranges that are over thousands of kilometers in scale (Davis and Campbell 1996; Takabayashi et al. 2002; Neuman et al. 2018; Rodriguez-Perez et al. 2020). The specific reproductive range of *Rugoconites* is unknown; however, the common occurrence of single or dispersed pairs of *Rugoconites* on surfaces is

not consistent with larval stages settling in locations relatively near conspecifics. The occurrence of solitary *Rugoconites* shows that they do not necessarily need to be near conspecifics such as certain species of barnacles or oysters (Rodríguez et al. 1993; Rodríguez-Perez et al. 2020).

Another possible cause of the aggregation of the *Rugoconites* on SE-Rugo is short dispersal/short-lived larval stage. Certain modern taxa, such as the soft coral *Alcyonium acaule*, have rapid-settling larvae produced via surface brooding (Ambroso et al. 2013). These corals have dense aggregated distributions but also a large ecological range, populating extensive portions of the Mediterranean Sea (Ambroso et al. 2013). However, examining dispersal limitations of an organism preserved on a surface that is only 3.6 m² is speculative and should be undertaken with caution. It is possible that *Rugoconites*, like numerous modern marine invertebrates, could reproduce both sexually and asexually. The aggregation of *Rugoconites* on SE-Rugo could result from unknown ecological or biological factor(s) that made the SE-Rugo surface ideal for settlement or a lack of post-settlement environmental filtering.

In contrast to *Rugoconites* and *Tribrachidium*, *Obamus* exhibits strong aggregation (best fit to a TC model; best-fit $pd = 0.556$), relatively low population density (5 individuals/m²), and a more selective environmental distribution. One possible explanation for this distribution is asexual reproduction. Another Ediacaran taxon, albeit from the older Avalon Assemblage, that fits a DTC is *Fractofusus*, which has been determined to have reproduced via stolons (Mitchell et al. 2015). There is no evidence at NENP of stolons in relation to *Obamus*, despite exceptional preservation on surfaces such as LV-FUN and TB-ARB, and the spatial scale for *Obamus* of 20 cm is significantly larger than those in which stoloniferous reproduction occurs (Mitchell et al. 2015). Despite evidence for quantitatively high intraspecific aggregation, no individuals have been found with edges touching, unlike several other sessile organisms at NENP, such as *Aspidella* or less commonly *Tribrachidium* (Hall et al. 2015; Tarhan et al. 2015b). The lack of touching among the hundreds of *Obamus* examined here suggests that asexual fission or budding is unlikely.

Instead, we propose that the selective nature of *Obamus* requires a dispersal mechanism that allows for some level of habitat preference. Previous studies of *Obamus* have noted its affinity for locations of mature microbial mat but no preference for mat type (Dzaugis et al. 2018; Droser et al. 2022). While pelagic larval stages are the most common type of dispersal for sessile benthic marine invertebrates, other reproductive strategies can result in habitat or range restrictions. In modern ecosystems, certain sponges have short dispersal ranges based on a combination of asexual budding and habitat preference that result in aggregated patterns (Lesneski et al. 2019). As was the case with *Rugoconites*, it is imprudent to attempt to predict the dispersal range of an organism using a surface limited to 22.4 m², when modern dispersal can range from centimeters to kilometers in scale (Jenkins 2005).

While an asexual model cannot be fully ruled out, the distribution of *Obamus* is also consistent with sexual reproduction. Selective larval stages are common among modern marine invertebrates that reproduce sexually, with planktonic larvae that are either transported or actively swim for days to months, navigating at small scales in order to secure a preferred substrate (Carlson and Olson 1993; Manríquez and Castilla 2007; Maldonado and Riesgo 2008; Denley et al. 2014; Chase et al. 2016; Wangensteen et al. 2016). These data do not suggest a swimming larval phase for *Obamus*; however, *Obamus* was not limited in its environmental dispersal range, occurring in two separate facies at NENP, reflecting environments between fair weather and storm wave base to a sub-wave base upper canyon fill (Droser et al. 2019). *Obamus* has not been found as a solitary individual on any surface at NENP, implying that at some scale, *Obamus* needed to be near conspecifics or had limited dispersal ranges. This, combined with a preference for specific substrates, could be responsible for the strong aggregation found on LV-FUN.

Tribrachidium is spatially variable, similar to *Aspidella* specimens from the Olenek Uplift and White Sea of Russia (although the types of variable spatial patterns differed; Mitchell et al. 2020). Aggregation, recorded in all three taxa here, was documented in *Funisia* and *Parvancorina* populations collected from the

Ediacara Hills, South Australia (Cou tts et al. 2018; Mitchell et al. 2020). The prevalence of aggregation for many of the White Sea taxa is consistent with modern marine benthic invertebrates, whose populations are often aggregated as a result of reproductive or environmental controls (e.g., Schmidt 1982; Keough 1984; Carlon and Olson 1993; Rodríguez et al. 1993; Miron et al. 1999; Manríquez and Castilla 2007; Ambroso et al. 2013; Hooper and Eichhorn 2016; Lesneski et al. 2019; De los Ríos and Carreño 2020; Rodríguez-Perez et al. 2020). Furthermore, *Charniodiscus* and *Fractofusus* from the Avalon Assemblage and *Ernietta* from the Nama Assemblage in Namibia (Gibson et al. 2019, 2021; Mitchell et al. 2019) have been shown to exhibit aggregation, indicating that this spatial pattern was present, or even common, throughout the Ediacara Biota.

While the pattern of aggregation is common throughout Ediacaran assemblages, the processes leading to these patterns differ by assemblage and taxa. In the Avalon Assemblage, spatial patterns are driven by random dispersal processes, while in the White Sea Assemblage, the dispersal method and environmental factors both play a role in distribution (Mitchell et al. 2015, 2019, 2020). Additionally, among Avalon taxa, spatial patterns and the processes that cause them are relatively consistent across different surfaces, which is not the case for White Sea taxa populations (e.g., the *Tribrachidium*; Mitchell et al. 2019). Finally, patterns in the Nama Assemblage have been reported as being a process of facilitation (Gibson et al. 2019). However, these observations require further work before any larger spatial ecological trends can be deduced from the three Ediacaran Assemblages.

Conclusions

The reproductive strategies of sessile marine invertebrates are vital to their spatial distributions. With the statistically viable populations examined here, it is possible to determine that different taxa at NENP had variable spatial distributions. These distributions also reflect key aspects of their life histories. In the case of *Tribrachidium*, we find that populations are best fit to the heterogenous Poisson or double Thomas cluster null models and are driven by either

environmental and/or dispersal processes. *Rugoconites* shows strong aggregation, but occur in low numbers on numerous beds. This pattern could be a function of reproductive methods in combination with settlement location availability at the time of dispersal and/or settlement. Additionally, post-settlement environmental controls could have resulted in the low specimen number on some surfaces. *Tribrachidium* and, to a lesser extent, *Rugoconites* are both possible examples of aggregation occurring when conditions were advantageous for dense settlement or outliers resulting from common post-settlement filtering on non-aggregated surfaces. *Obamus* is an example of a strongly aggregated organism that only occurs with conspecifics and in locations of mature microbial mats. This dispersal process is the first example of a member of the Ediacara Biota that was substrate selective, something commonly found throughout modern invertebrate populations.

Acknowledgments

Thanks are extended to the Department of Environment and Water of the South Australia government and to R. Fargher and J. Fargher for access to the NENP. We acknowledge that this land lies within the Adnyamathanha Traditional Lands. Additionally, we acknowledge that the University of California, Riverside (where the majority of lab work was done) lies within the traditional lands of the Cahuilla, Tongva, Luiseño, and Serrano Peoples. H. McCandless assisted in the logging of TBEW and creation of photogrammetric 3D models. We thank A. Kovalick, A. Rizzo, W. Weyland, and R. Surprenant for their helpful discussions. T. Wiegand provided helpful suggestions and explanations regarding SPPA methodology. Fieldwork was facilitated by P. Dzaugis, I. Hughes, and E. Hughes. N. Tam, G. M. Boan, and M. Figueroa aided in the preparation of this article. This project was funded by the NASA Exobiology Program (NASA grant NNG04GJ42G) to M.L.D., a student research grant from the Society for Sedimentary Geology awarded to P.C.B., a Lerner-Gray Memorial Fund for Marine Research grant from the American Museum of Natural History awarded to P.C.B., a CARES grant from the Geological

Society of America awarded to P.C.B., an N. Gary Lane Student Research Award grant from the Paleontological Society awarded to P.C.B., and an NSF/GSA Graduate Student Geoscience grant no. 13053-21, which is funded by NSF Award no. 1949901 awarded to P.C.B. This paper benefited greatly from reviews by E. Mitchell and an anonymous reviewer.

Declaration of Competing Interests

The authors declare no competing interests.

Data Availability Statement

Data available from the Dryad Digital Repository: <https://doi.org/10.6086/D1M67C>.

Literature Cited

- Ambroso, S., A. Gori, C. Dominguez-Carrió, J. Gill, E. Berganzo, N. Teixidó, M. Greenacre, and S. Rossi. 2013. Spatial distribution patterns of the soft corals *Alcyonium acaule* and *Alcyonium palmatum* in coastal bottoms (Cap de Creus, northwestern Mediterranean Sea). *Marine Biology* 160:3059–3070.
- Atkinson, P. M., G. M. Foody, P. W. Gething, A. Mathur, and C. K. Kelly. 2007. Investigating spatial structure in specific tree species in ancient semi-natural woodland using remote sensing and marked point pattern analysis. *Ecography* 30:88–104.
- Baddeley, A., E. Rubak, and R. Turner. 2016. *Spatial point patterns: methodology and applications with R*. Chapman and Hall Books, Boca Raton, Fla.
- Ben-Said, M. 2021. Spatial point-pattern analysis as a powerful tool in identifying pattern-process relationships in plant ecology: an updated review. *Ecological Processes* 10:1–23.
- Boag, T. H., S. A. F. Darroch, and M. Laflamme. 2016. Ediacaran distributions in space and time: testing assemblage concepts of earliest macroscopic body fossils. *Paleobiology* 42:574–594.
- Bobrovskiy, I., J. M. Hope, A. Ivantsov, B. J. Nettersheim, C. Hallman, and J. J. Brocks. 2018. Ancient steroids establish the Ediacaran fossil *Dickinsonia* as one of the earliest animals. *Science* 361:1246–1249.
- Brenchley, P. J. and D. A. T. Harper. 1998. *Palaeoecology: ecosystems, environments and evolution*. Chapman and Hall, London.
- Carlson, D. B., and R. R. Oslen. 1993. Larval dispersal distance as an explanation for adult spatial pattern in two Caribbean reef corals. *Journal of Experimental Marine Biology and Ecology* 173:247–263.
- Carrer, M., D. Castagneri, I. Popa, M. Pividori, and E. Lingua. 2018. Tree spatial patterns and stand attributes in temperate forests: the importance of plot size, sampling design, and null model. *Forest Ecology and Management* 407:125–134.
- Chang, C. Y., and D. J. Marshall. 2016. Spatial pattern of distribution of marine invertebrates within a subtidal community: do communities vary more among patches or plots? *Ecology and Evolution* 6:8330–8337.
- Chase, A. L., J. A. Dijkstra, and L. G. Harris. 2016. The influence of substrate material on ascidian larval settlement. *Marine Pollution Bulletin* 106:35–42.
- Clapham, M. E., G. M. Narbonne, and J. G. Gehling. 2003. Paleoeecology of the oldest known animal communities: Ediacaran assemblages at Mistaken Point, Newfoundland. *Paleobiology* 29:527–544.
- Coutts, F. J., C. J. A. Bradshaw, D. C. García-Bellido, and J. G. Gehling. 2018. Evidence of sensory-driven behavior in the Ediacaran organism *Parvancorina*: implications and autecological interpretations. *Gondwana Research* 55:21–29.
- Cunningham, J. A., A. G. Liu, S. Bengtson, and P. C. J. Donoghue. 2017. The origin of animals: can molecular clocks and the fossil record be reconciled. *Bioessays* 39:1–17.
- Darroch, S. A. F., M. Laflamme, and M. E. Clapham. 2013. Population structure of the oldest known macroscopic communities from Mistaken Point, Newfoundland. *Paleobiology* 39:591–608.
- Darroch, S. A. F., I. A. Rahman, B. Gibson, R. A. Racicot, and M. Laflamme. 2017. Inference of facultative mobility in the enigmatic Ediacaran organism *Parvancorina*. *Biology Letters* 13:0170033.
- Davis, A. R., and D. J. Campbell. 1996. Two levels of spacing and limits to local population density for settled larvae of the ascidian *Clavelina moluccensis*: a nearest-neighbour analysis. *Oecologia* 108:701–707.
- De los Ríos, P. and E. Carreño. 2020. Spatial distribution in marine invertebrates in rocky shore of Araucanía Region (38° S, Chile). *Brazilian Journal of Biology* 80:362–367.
- Denley, D., A. Metaxas, and J. Short. 2014. Selective settlement by larvae of *Membranipora membranacea* and *Electra pilosa* (Ectoprocta) along kelp blades in Nova Scotia, Canada. *Aquatic Biology* 21:47–56.
- Dhungana, A., and E. G. Mitchell. 2021. Facilitating corals in an early Silurian deep-water assemblage. *Palaeontology* 64:359–370.
- Droser, M. L., and J. G. Gehling. 2008. Synchronous aggregate growth in an abundant new Ediacaran tubular organism. *Science* 319:1660–1662.
- Droser, M. L., L. G. Tarhan, and J. G. Gehling. 2017. The rise of animals in a changing environment: global ecological innovation in the late Ediacaran. *Annual Review of Earth and Planetary Sciences* 45:593–617.
- Droser, M. L., J. G. Gehling, L. G. Tarhan, S. D. Evans, C. M. S. Hall, I. V. Hughes, E. B. Hughes, M. E. Dzaugis, M. P. Dzaugis, P. W. Dzaugis, and D. Rice. 2019. Piecing together the puzzle of the Ediacara Biota: excavation and reconstruction at the Ediacara National Heritage site Nilpena (South Australia). *Paleogeography, Paleoclimatology, Palaeoecology* 23:181–194.
- Droser, M. L., L. G. Tarhan, S. D. Evans, R. L. Surprenant, and J. G. Gehling. 2020. Biostratigraphy of the Ediacara Member (Rawnsley Quartzite, South Australia): implications for depositional environments, ecology and biology of Ediacara organisms. *Interface Focus* 10: 20190100.
- Droser, M. L., S. D. Evans, L. G. Tarhan, R. L. Surprenant, I. V. Hughes, E. B. Hughes, and J. G. Gehling. 2022. What happens between depositional events, stays between depositional events: the significance of organic mat surfaces in the capture of Ediacara communities and the sedimentary rocks that preserve them. *Frontiers in Earth Science* 10. doi: 10.3389/feart.2022.826353.
- Dunn, F. S., A. G. Liu, and P. C. J. Donoghue. 2018. Ediacaran developmental biology. *Biological Reviews* 93:914–932.
- Dunn, F. S., A. G. Liu, D. V. Grazhdankin, P. Vixseboxse, J. Flannery-Sutherland, E. Green, S. Harris, P. R. Wilby, and P. C. Donoghue. 2021. The developmental biology of *Charnia* and the eumetazoan affinity of the Ediacaran rangeomorphs. *Science Advances* 7:eabe0291.
- Dunn, F. S., C. G. Kenchington, L. A. Parry, J. W. Clark, R. S. Kendall, and P. R. Wilby. 2022. A crown-group cnidarian from the Ediacaran of Charnwood Forest. *Nature Ecology and Evolution* 6:1095–1104.
- Dzaugis, P. W., S. D. Evans, M. L. Droser, J. G. Gehling, and I. V. Hughes. 2018. Stuck in the mat: *Obamus coronatus*, a new benthic organism from the Ediacara Member, Rawnsley Quartzite, South Australia. *Australian Journal of Earth Sciences* 67:1–7.

- Erwin, D. H. 2015. Novelty and innovation in the history of life. *Current Biology* 25: R930–R940.
- Erwin, D. H. 2021. The origin of animal body plans: a view from fossil evidence and the regulatory genome. *Development* 147: dev182899.
- Erwin D. H., and J. W. Valentine. 2013. *The Cambrian Explosion: The Construction of Animal Biodiversity*. Roberts & Co, Greenwood, Colo.
- Evans, S. D., J. G. Gehling, and M. L. Droser. 2019. Slime travelers: early evidence of animal mobility and feeding in a organic mat world. *Geobiology* 17:490–509.
- Evans, S. D., P. W. Dzaugis, M. L. Droser, and J. G. Gehling. 2020a. You can get anything you want from Alice's Restaurant Bed: exceptional preservation and an unusual fossil assemblage from a newly excavated bed (Ediacara Member, Nilpena, South Australia). *Australian Journal of Earth Science* 67:873–883.
- Evans, S. D., I. V. Hughes, J. G. Gehling, and M. L. Droser. 2020b. Discovery of the oldest bilaterian from the Ediacaran of South Australia. *Proceedings of the National Academy of Sciences USA* 117:7845–7850.
- Evans, S. D., M. L. Droser, and D. H. Erwin. 2021a. Developmental processes in Ediacara macrofossils. *Proceedings of the Royal Society of London B* 288:20203055.
- Evans, S. D., J. G. Gehling, D. H. Erwin, and M. L. Droser. 2021b. Ediacara growing pains: modular addition and development in *Dickinsonia costata*. *Paleobiology* 48:83–98.
- Fedonkin, M. A. 1984. Promorphology of Vendian Radialia. Pp. 49–50 in A. B. Ivanovsky and I. B. Ivanov, eds. *Stratigraphy and paleontology of the most ancient Phanerozoic*. Nauka, Moscow. [In Russian.]
- Franklin, J., and E. V. Santos. 2010. A spatially explicit census reveals population structure and recruitment patterns for a narrowly endemic pine, *Pinus torreyana*. *Plant Ecology* 212:293–306.
- Gehling, J. G. 1999. Microbial mats in terminal Proterozoic siliciclastics: Ediacaran death masks. *Palaios* 14:40–57.
- Gehling, J. G. 2000. Environmental interpretation and a sequence stratigraphic framework for the terminal Proterozoic Ediacara Member within the Rawnsley Quartzite, South Australia. *Precambrian Research* 100:65–95.
- Gehling, J. G., and M. L. Droser. 2009. Textured organic surfaces associated with the Ediacara biota in South Australia. *Earth-Science Reviews* 96:196–206.
- Gehling, J. G., and M. L. Droser. 2013. How well do fossil assemblages of the Ediacara Biota tell time. *Geology* 41:447–450.
- Gehling, J. G., and M. L. Droser. 2018. Ediacaran scavenging as a prelude to predation. *Emerging Topics in Life Sciences* 2:213–222.
- Gehling, J. G., D. C. García-Bellido, M. L. Droser, L. G. Tarhan, and B. Runnegar. 2019. The Ediacaran–Cambrian transition: sedimentary facies versus extinction. *Estudios Geológicos* 75:e099.
- Gibson, B. M., I. A. Rahman, K. M. Maloney, R. A. Racicot, H. Mocke, M. Laflamme, and S. A. F. Darroch. 2019. Gregarious suspension feeding in a modular Ediacaran organism. *Science Advances* 5:eaaw0260.
- Gibson, B. M., S. A. F. Darroch, K. M. Maloney, and M. Laflamme. 2021. The importance of size and location within gregarious populations of *Ernieitia plateauensis*. *Frontiers in Earth Science* 9. doi: 10.3389/feart.2021.749150.
- Glaessner, M. F., and B. Daily. 1959. The geology and late Precambrian fauna of the Ediacara Fossil Reserve. *Records of the South Australia Museum* 13:396–401.
- Glaessner, M. F. and M. Wade. 1966. The Late Precambrian fossils from Ediacara, South Australia. *Palaeontology* 9:599–628.
- Grazhdankin, D. V., and A. Yu. Ivantsov. 1995. Reconstructions of biotopes of ancient metazoa of the Late Vendian White Sea Biota. *Paleontological Journal* 30:674–678.
- Guy-Haim, T., G. Rilov, and Y. Aчитuv. 2015. Different settlement strategies explain intertidal zonation of barnacles in the Eastern Mediterranean. *Journal of Experimental Marine Biology and Ecology* 463:125–134.
- Hall, C. M. S., M. L. Droser, J. G. Gehling, and M. E. Dzaugis. 2015. Paleocology of the enigmatic *Tribrachidium*: a new data from the Ediacaran of South Australia. *Precambrian Research* 269:183–194.
- Hall, C. M. S., M. L. Droser, and J. G. Gehling. 2018. Sizing up *Rugocmites*: a study of the ontogeny and ecology of an enigmatic Ediacaran genus. *AP Memoirs* 51:7–17.
- Harms, K. E., S. J. Wright, O. Calderon, A. Hernandez, and E. A. Herre. 2000. Pervasive density-dependent recruitment enhances seedling diversity in a tropical forest. *Nature* 40:493–495.
- He, F., and P. Legendre. 2002. Species diversity patterns derived from species-area models. *Ecology* 83:1185–1198.
- Hooper, R. C., and M. P. Eichhorn. 2016. Too close for comfort: spatial patterns in acorn barnacle populations. *Population Ecology* 58:231–239.
- Illian, J., A. Penttinen, H. Stoyan, and D. Stoyan. 2008. *Statistical analysis of modelling of spatial point patterns*. Wiley, Chichester, U.K.
- Ivantsov, A. Yu., and M. A. Zakrevskaya. 2021. Trilobozoa, Precambrian tri-radial organisms. *Paleontological Journal* 55:727–741.
- Jaquemyn, H., R. Brys, K. Vandepitte, O. Honnay, I. Roldan-Ruiz, and T. Wiegand. 2007. A spatially explicit analysis of seedling recruitment in the terrestrial orchid *Orchis purpurea*. *New Phytologist* 176:448–459.
- Jenkins, S. R. 2005. Larval habitat selection, not larval supply, determines settlement patterns and adult distribution in two chthamaliid barnacles. *Journal of Animal Ecology* 79:793–904.
- Karlson, R. H., T. P. Hughes, and S. R. Karlson. 1996. Density-dependent dynamics of soft coral aggregations: the significance of clonal growth and form. *Ecology* 77:1592–1599.
- Kenkel, N. C. 1988. Pattern of self-thinning in jack pine: testing the random mortality hypothesis. *Ecology* 69:1017–1024.
- Keough, M. J. 1984. Kin-Recognition and the spatial distribution of larvae of the bryozoan *Bugula neritina* (L.). *Evolution* 38:142–147.
- Laflamme, M., S. Xiao, and M. Kowalewski. 2009. Osmotrophy in modular Ediacara organisms. *Proceedings of the National Academy of Sciences USA* 106:14438–14443.
- Law, R., J. Illian, D. F. R. P. Burslem, G. Gratzler, C. V. S. Gunatilleke, and I. A. U. N. Gunatilleke. 2009. Ecological information from spatial patterns of plants: insight from point process theory. *Journal of Ecology* 97:616–628.
- Lesneski, K. C., C. C. D'Aloia, M. J. Fortin, and P. M. Buston. 2019. Disentangling the spatial distributions of a sponge-dwelling fish and its host sponge. *Marine Biology* 166:1–8..
- Lin, Y., L. Chang, K. Yang, H. Wang, and I. Sun. 2011. Point patterns of tree distribution determined by habitat heterogeneity and dispersal limitation. *Oecologia* 165:175–184.
- Maldonado, M., and A. Riesgo. 2008. Reproduction in the phylum Porifera: a synoptic overview. *Treballs de la SCB* 59:29–49.
- Mallison, H., and O. Wings. 2014. *Photogrammetry in paleontology — a practical guide*. *Journal of Paleontological Techniques* 12:1–3.
- Manríquez, P. H., and J. C. Castilla. 2007. Roles of larval behaviour and microhabitat traits in determining spatial aggregations in the ascidian *Pyura chilensis*. *Marine Ecology Progress Series* 332:155–165.
- Martin, M. W., D. V. Grazhdankin, S. A. Bowring, D. A. D. Evans, M. A. Fedonkin, and J. L. Kirschvink. 2000. Age of Neoproterozoic bilaterian body and trace fossils, White Sea, Russia: implications for metazoan evolution. *Science* 288:841–845.
- Miron, G., B. Boudreau, and E. Bourget. 1999. Intertidal barnacle distribution: a case study using multiple working hypotheses. *Marine Ecology Progress Series* 189:205–219.
- Mitchell, E. G., and N. J. Butterfield. 2018. Spatial analyses of Ediacaran communities at Mistaken Point. *Paleobiology* 44:40–57.
- Mitchell, E. G., and S. Harris. 2020. Mortality, population and community dynamics of the glass sponge dominated community “the forest of the weird” from the Ridge Seamount, Johnston Atoll, Pacific Ocean. *Frontiers in Marine Science* 7:1–21.

- Mitchell, E. G. and C. G. Kenchington. 2018. The utility of height for the Ediacaran organisms of Mistaken Point. *Nature Ecology and Evolution* 2:1218–1222.
- Mitchell, E. G., C. G. Kenchington, A. G. Liu, J. J. Matthews, and N. J. Butterfield. 2015. Reconstructing the reproductive mode of an Ediacaran macro-organism. *Nature Letters* 524:343–346.
- Mitchell, E. G., C. G. Kenchington, S. Harris, and P. R. Wilby. 2018. Revealing rangeomorph species characters using spatial analysis. *Canadian Journal of Earth Sciences* 55:1262–1270.
- Mitchell, E. G., S. Harris, C. G. Kenchington, P. Vixeboxse, L. Robers, C. Clark, A. Dennis, A. G. Liu, and P. R. Wilby. 2019. The importance of neutral over niche processes in structuring Ediacaran early animal communities. *Ecology Letters* 22:2028–2038.
- Mitchell, E. G., N. Bobkov, N. Bykova, A. Dhungana, A. V. Kolesnikov, I. R. P. Hogarth, A. G. Liu, T. M. R. Mustill, N. Sozonov, V. I. Rogov, S. Xiao and D. V. Grazhdankin. 2020. The influence of environmental setting on the community ecology of Ediacaran organisms. *Interface Focus* 10:1–14.
- Mitchell, E. G., S. D. Evans, Z. Chen, and S. Xiao. 2022. A new approach for investigating spatial relationships of ichnofossils: a case study of Ediacaran–Cambrian animal traces. *Paleobiology* 48:557–575.
- Narbonne, G. M., and H. J. Hofmann. 1987. Ediacaran Biota of the Wernecke Mountains, Yukon, Canada. *Paleontology* 30:647–676.
- Neuman, M. J., S. Wang, S. Busch, C. Friedman, K. Gruenthal, R. Gustafson, D. Kushner, K. Stierhoff, G. Vanblaricom, and S. Wright. 2018. A status review of Pinto Abalone (*Haliotis kamtschakana*) along the west coast of North America: interpreting trends, addressing uncertainty, and assessing risk for a wide-ranging marine invertebrate. *Journal of Shellfish Research* 37:869–910.
- Pawlik, J. R. 1992. Chemical ecology of the settlement of benthic marine invertebrates. *Oceanography and Marine Biology: An Annual Review* 30:273–335.
- Rahman, I. A., S. A. F. Darroch, R. A. Racicot, and M. Laflamme. 2015. Suspension feeding in the enigmatic Ediacaran organism *Tribrachidium* demonstrates complexity of Neoproterozoic ecosystems. *Science Advances* 1:1–8.
- Rodríguez, S. R., F. P. Ojeda, and N. C. Inestrosa. 1993. Settlement of benthic marine invertebrates. *Marine Ecology Progress Series* 97:193–207.
- Rodríguez-Perez, A., W. G. Sanderson, L. F. Møller, T. B. Henry, and M. James. 2020. Return to sender: the influence of larval behaviour on the distribution and settlement of the European oyster *Ostrea edulis*. *Aquatic Conservation: Marine and Freshwater Ecosystems* 30:2116–2132.
- Rossi, S., and M. J. Snyder. 2001. Competition for space among sessile marine invertebrates: changes in HSP70 expression in two Pacific cnidarians. *Biological Bulletin* 201:385–393.
- Sampayo, E. M., G. Roff, C. A. Sims, P. G. Rachello-Dolmen, and J. M. Pandolfi. 2020. Patch size drives settlement success and spatial distribution of coral larvae under space limitation. *Coral Reefs* 39:387–396.
- Schleicher, J., K. M. Meyer, K. Wiegand, F. M. Schurr, and D. Ward. 2011. Disentangling facilitation and seed dispersal from environmental heterogeneity as mechanisms generating associations between savanna plants. *Journal of Vegetation Science* 22:1038–1048.
- Schmidt, G. H. 1982. Random and aggregative settlement in some sessile marine invertebrates. *Marine Ecology Progress Series* 9:97–100.
- Surprenant, R. L., J. G. Gehling, and M. L. Droser. 2020. Biological and ecological insights from the preservational variability of *Funi-sia dorothea*, Ediacara Member, South Australia. *Palaios* 35:359–376.
- Takabayashi, M., D. A. Carter, J. V. Lopez, and O. Hoegh-Guldberg. 2002. Genetic variation of the scleractinian coral *Stylophora pistillata*, from western Pacific reefs. *Coral Reefs* 22:17–22.
- Tarhan, L. G., M. L. Droser, and J. G. Gehling. 2015a. Depositional and preservational environments of the Ediacara Member, Rawnsley Quartzite (South Australia): Assessment of paleoenvironmental proxies and the timing of “ferruginization.” *Paleogeography, Paleoclimatology, Palaeoecology* 434:4–13.
- Tarhan, L. G., M. L. Droser, J. G. Gehling, and M. P. Dzaugis. 2015b. Taphonomy and morphology of the Ediacaran form genus *Aspidella*. *Precambrian Research* 256:124–136.
- Tarhan, L. G., M. L. Droser, J. G. Gehling, and M. P. Dzaugis. 2017. Microbial mat sandwiches and other anactulistic sedimentary features of the Ediacara Member (Rawnsley Quartzite, South Australia): implications for interpretation of the Ediacaran sedimentary record. *Palaios* 32:181–194.
- Tarhan, L. G., M. L. Droser, and J. G. Gehling. 2022. Picking out the warp and weft of the Ediacaran seafloor: Paleoenvironment and paleoecology of an Ediacara textured organic surface. *Precambrian Research* 369:106539.
- Velázquez, E., I. Martínez, S. Getzin, K. A. Moloney, and T. Wiegand. 2016. An evaluation of the state of spatial point pattern analysis in ecology. *Ecography* 39:1042–1055.
- Vixeboxse, P. B., C. G. Kenchington, F. S. Dunn, and E. G. Mitchell. 2021. Orientations of Mistaken Point fronds indicate morphology impacted ability to survive turbulence. *Frontiers in Earth Science* 9:762824.
- Wangensteen, O. S., X. Turon, and C. Placín. 2016. Reproductive strategies in marine invertebrates and the structuring of marine animal forests. Pp. 571–594 in S. Rossi, L. Bramanti, A. Gori, and C. Orejas, eds. *Marine animal forests*. Springer, Cham, Switzerland.
- Watson, D. M., D. A. Roshier, and T. Wiegand. 2007. Spatial ecology of a root parasite—from pattern to process. *Austral Ecology* 32:359–369.
- Wiegand, T., and K. A. Moloney. 2004. Rings, circles, and null-models for point pattern analysis in ecology. *OIKOS* 104:209–229.
- Wiegand, T., and K. A. Moloney. 2014. *Handbook of spatial point-pattern analysis in ecology*. Chapman and Hall, Boca Raton, Fla.
- Wiegand, T., D. Kissling, P. A. Cipriotti, and M. R. Aguiar. 2006. Extending point pattern analysis for objects of finite size and irregular shape. *Journal of Ecology* 94:827–837.
- Wiegand, T., S. Gunatilleke, and N. Gunatilleke. 2007a. Species associations in a heterogeneous Sri Lankan dipterocarp forest. *American Naturalist* 170:E77–E95.
- Wiegand, T., S. Gunatilleke, N. Gunatilleke, and T. Okuda. 2007b. Analyzing the spatial structure of a Sri Lankan tree species with multiple scales of clustering. *Ecology* 88:3088–3102.
- Wiegand, T., I. Martínez, and A. Huth. 2009. Recruitment in tropical tree species: revealing complex spatial patterns. *American Naturalist* 175:E106–E120.
- Wiegand, T., P. Grabarnik, P., and Stoyan, D. 2016. Envelope tests for spatial point patterns with and without simulation. *Ecosphere* 7:e01365.
- Zakrevskaya, M. 2014. Paleocological reconstruction of the Ediacaran benthic macroscopic communities of the White Sea (Russia). *Paleogeography, Paleoclimatology, Palaeoecology* 410:27–38.
- Zillio, T., and F. He. 2010. Modeling spatial aggregation of finite populations. *Ecology* 92:3698–3706.